



COVID-19 Classification Algorithm Based on Privacy Preserving Federated Learning

Changqing Ji^{1,2}, Cheng Baoluo², Gao Zhiyong², Qin Jing³, and Wang Zumin²(✉)

¹ College of Physical Science and Technology, Dalian University, Dalian 116622, Liaoning, China

² College of Information Engineering, Dalian University, Dalian 116622, Liaoning, China
wangzumin@163.com

³ School of Software Engineering, Dalian University, Dalian 116622, Liaoning, China

Abstract. In order to solve the problems of complex feature extraction, slow convergence of model and most of the deep learning based COVID-19 classification algorithms ignore the problem of “island” of medical data and security. We innovatively propose a COVID-19 X-ray images classification algorithm based on federated learning framework, which integrates hybrid attention mechanism and residual network. The algorithm uses hybrid attention mechanism to highlight high-resolution features with large channel and spatial information. The average training time is introduced to avoid the long-term non-convergence of the local model and accelerate the convergence of the global model. For the first time, we used the federated learning framework to conduct distributed training on COVID-19 detection, effectively addressing the data “islands” and data security issues in healthcare institutions. Experimental results show that the Accuracy, Precision, Sensitivity and Specific of the proposed algorithm for COVID-19 classification on datasets named ‘ COVID-19 Chest X-ray Database’ can reach 0.939, 0.921, 0.928 and 0.947, respectively. The convergence time of the global model is shortened by about 30 min. That improves the performance and training speed of the COVID-19 X-ray image classification model with privacy security.

Keywords: Federated learning · COVID-19 · Convolutional block attention module · Resnet50 · Privacy preserving

1 Introduction

Corona Virus Disease-2019 (COVID-19), has been rampant around the world since the outbreak in 2019, and according to WHO statistics, the number of people diagnosed worldwide has exceeded 625 million by October 26, 2022, and the number of deaths has exceeded 6.56 million. A large number of them died due to severe lung infection found late, so it is particularly important to detect COVID-19 patients as early as possible. X-ray has become a key screening method for the early detection of COVID-19 due to its wide penetration rate, low cost and high accuracy [1]. Doctors will be able to analyze the X-ray images to determine if the patient has been diagnosed with COVID-19.

Currently, the success of Deep Learning (DL) in image detection has made it an important technology for computer-aided medical applications, which can help doctors analyze chest X-rays to make quick judgments. Deep learning needs a large amount of training data with strong differences to train a deep learning model with high accuracy and strong robustness. However, because the privacy and security of data has been paid more and more attention around the world, various countries have introduced various laws and regulations to regulate and protect data security. In May 2018, the EU issued the General Data Protection Regulation (GPR) Act for data protection; On September 1, 2021, the Data Security Law of the People's Republic of China was officially put into effect. So specific medical data from the hospital is not allowed to be leaked, and collecting training data that meets the requirements is a major challenge.

Federated Learning (FL) [2] is an effective method to solve the problem of data collection. In 2017, it was proposed by H.Brendan McMahan and others from Google. As a privacy preserving distributed machine learning technology, it can deploy deep learning algorithm in each client and use local data to train the model. Then the model is aggregated by the central server and redistributed to each client for training. In this way, it can ensure that the data is not out of local clients, the cooperation between the client training model, and comply with the data security protection related treaties.

Some scholars have noted data security issues. Psychoula I. et al. [3, 4] consider privacy preservation in deep learning. Yao X. et al. [5] found privacy issues of physical objects in the IoT. Some scholars proposed to introduce federated learning for neural network model training. Pfohl et al. [6] proposed distributed privacy learning for EMR in the federated environment, and they further proved that the performance of this model can be comparable to that of centralized training. Dayan et al. [7] used a federal learning framework to provide data of COVID-19 patients from more than 20 institutions around the world. The model input patients' vital signs, laboratory data and chest X-ray. Predict the vital signs of a symptomatic COVID-19 patient from presentation to the next 72 h. Feki et al. [8] proposed a federated learning framework based on deep convolutional neural network (VGG16 and ResNet50) for COVID-19 detection in chest X-ray images. Zhang et al. [9] designed a federated learning system model based on dynamic fusion for the analysis and detection of CT scan or X-ray images of COVID-19 patients. Liu et al. [10] compared the performance of four different network models (MobileNet, ResNet18, MoblieNet and covid) using the federated learning framework.

Aiming at the existing problems and development status of existing models, we propose a COVID-19 X-ray image classification algorithm (FL-Resnet-CBAM) based on federated learning with hybrid attention mechanism and residual network. Mainly has the following three innovations:

1. Proposed distributed training of COVID-19 classification model in federated learning framework to effectively solve the data "island" problem and user privacy security problem in medical institutions.
2. Improve the Resnet network and add the mixed attention mechanism into the Resnet network, which significantly improves the model detection accuracy.
3. Optimize the federated learning framework and introduce the average training time of local models in the training process, which can prevent the global model from not converging for a long time. The AdaGrad optimizer is used to make use of sparse

gradient information in discrete clients to achieve more efficient convergence of the model.

2 Related Work

2.1 Residual Network

He et al. [11] put forward such as not changing input by convolution layer at the same time increase the same mapping makes input directly mapped to the output of the nonlinear layer, namely the residual network. There are five stages in the Resnet50 network, as shown in Fig. 1. Stage1 is mainly a preprocessing operation. Residual modules in Stage2-Stage5 include mapping module Identity Block (Id Block) and Convolution Block (Conv Block). The dimension of input and output vectors of Id Block are the same, and the network can be deepened directly through series. Learn deep semantic information. The dimensions of the input and output vectors of Conv Block are different, and 1×1 convolution should be performed to match the dimensions.

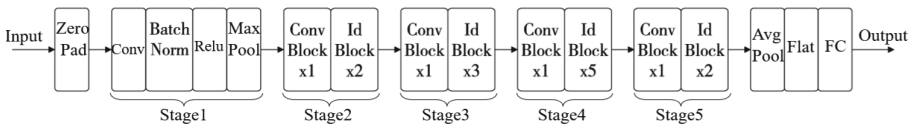


Fig. 1. Resnet50 Network structure

2.2 Hybrid Attention Mechanism

Hybrid attention mechanism refers to the comprehensive evaluation of Channel Attention Module (CAM) and spatial Attention Module (Spatial Attention Module (SAM) simultaneously. Convolutional Block Attention Module (CBAM) [12] is shown in Fig. 2.

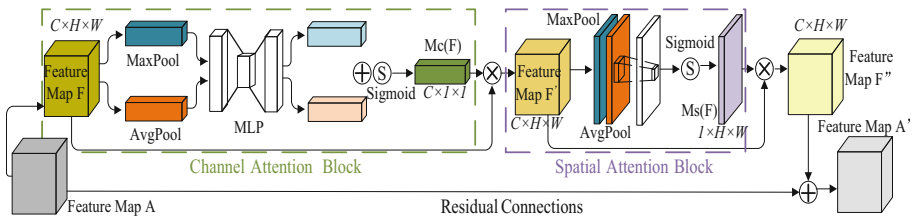


Fig. 2. Hybrid Attention Block CBAM structure

Channel attention module will input feature map $F (H \times W \times C)$ through global max pooling and global average pooling based on width and height respectively to obtain different spatial semantic description operators. Then they are fed into a two-layer shared neural network (MLP) with ReLU function as activation function. Then, the feature map

output by MLP is added and activated by sigmoid to generate channel attention feature, namely $\mathbf{M}_c(\mathbf{F})$, formula (1). Then, $\mathbf{M}_c(\mathbf{F})$ is multiplied with the input feature map \mathbf{F} to obtain the feature map \mathbf{F}' containing channel attention.

$$\mathbf{M}_c(\mathbf{F}) = \sigma\left(\mathbf{W}_1\left(\mathbf{W}_0\left(\mathbf{F}_{\text{avg}}^c\right)\right) + \mathbf{W}_1\left(\mathbf{W}_0\left(\mathbf{F}_{\text{max}}^c\right)\right)\right) \quad (1)$$

σ is sigmoid, $W_0 = \frac{C}{r} \times C$, $W_1 = C \times \frac{C}{r}$.

The spatial attention module takes the feature map \mathbf{F}' output from the channel attention module as the input feature map. Two $H \times W \times 1$ feature maps are obtained by global max pooling and global average pooling operations along the channel dimension. Concat operation is performed on these two feature maps based on channels, and then a convolution operation with a convolution kernel of 7×7 is performed. The dimension is reduced to one channel $H \times W \times 1$, and then the spatial attention feature, namely $\mathbf{M}_s(\mathbf{F})$, formula (2). The input feature map \mathbf{F}' of $\mathbf{M}_s(\mathbf{F})$ module is multiplied to obtain the feature map \mathbf{F}'' including channel attention and spatial attention.

$$\mathbf{M}_s(\mathbf{F}) = \sigma\left(f^{7 \times 7}\left(\left[\mathbf{F}_{\text{avg}}^s; \mathbf{F}_{\text{max}}^s\right]\right)\right) \quad (2)$$

σ is sigmoid function, and $f^{7 \times 7}$ is convolution operation with filter size 7×7 .

3 FL-Resnet-CBAM Classification Algorithm

3.1 General Framework of FL-Resnet-CBAM

In this paper, an image classification algorithm based on federated learning and deep residual network fusion hybrid attention mechanism (namely FL-Resnet-CBAM) is proposed to realize the recognition of COVID-19 images. The overall algorithm flowchart is shown in Fig. 3.

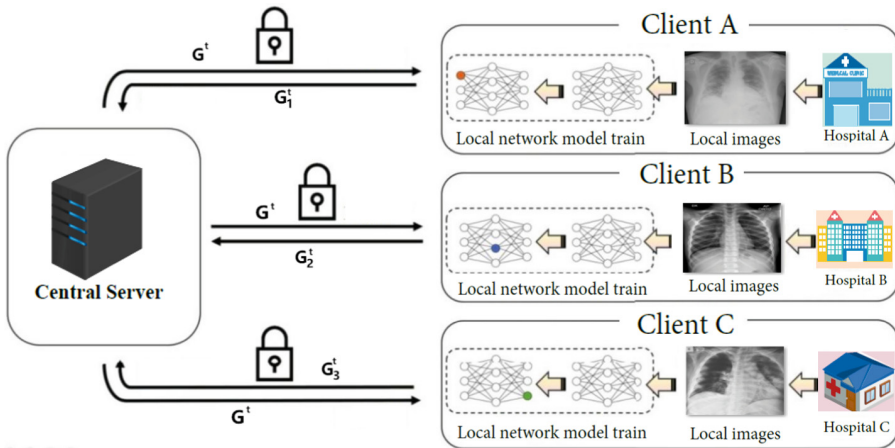


Fig. 3. FL-Resnet-CBAM algorithm framework

In this paper, the centralized aggregation method is adopted to do horizontal federation learning and training, which is mainly composed of aggregation server and multiple discrete clients. Two-way communication can be conducted between server and client, but each client cannot initiate communication. The federated server can use a cloud server, and the local client can be a discrete healthcare facility. The server plays the role of distributing and aggregating models, and the client plays the role of receiving models and training local models. The improved Resnet network model is deployed in each client, and the data used for model training is independent and distributed. The local data in each institution consists of different numbers and types of COVID-19 X-ray images.

3.2 Improved Resnet50 Network

The original Resnet50 residual network, after performing a 5-stage residual convolution operation, was directly and fully connected for classification, but the accuracy on classification of new coronary pneumonia images was obviously not sufficient.

The CBAM module adopts the method of serial channel attention and spatial attention, that is, the feature map F is first corrected by channel attention to F' , and then F' is corrected by spatial attention. Through this module, the model can learn what information in the image and where features need to be emphasized or suppressed, which can effectively help the information flow in the network and enhance feature extraction. The combination of channel attention and spatial attention can save parameters and computational power and can be easily integrated into the existing network architecture.

On basis of the original Resnet50, the mixed-domain attention module CBAM is added, as shown in Fig. 4. Specifically, the CBAM module is embedded in the last convolutional layer of Stage5, and the residual structure is introduced into the model with the embedded attention mechanism, which can effectively suppress the problems of gradient explosion and network degradation. The advantage of embedding CBAM module in the last layer is that the pre-training parameters of Resnet50 model can be used to accelerate the convergence of the training model.

3.3 The Training Flow and Optimization of FL-Resnet-CBAM

In the model training, the initial training parameters are first distributed to all clients, and k clients are randomly selected from the current client set N to participate in the training. In each round of training, the server selects only some clients to participate, which can improve the convergence speed of the local model and accelerate the convergence of the global model.

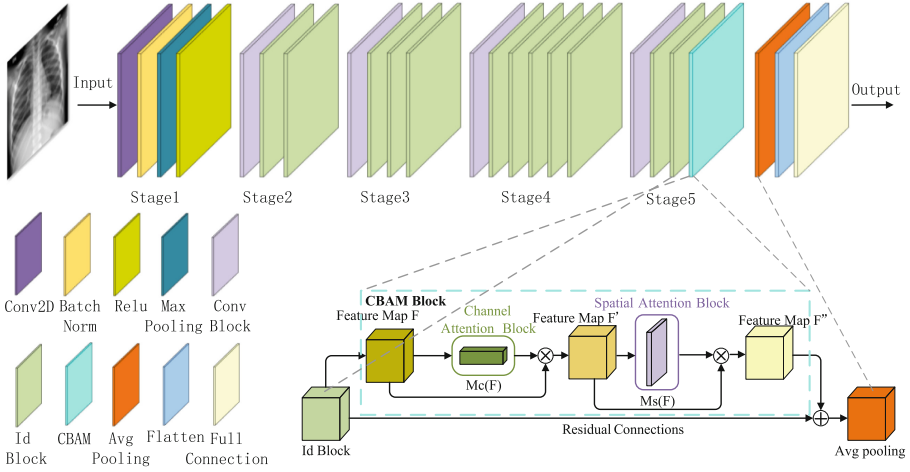


Fig. 4. Improved Resnet50 network structure

Considering the problem that the local model does not converge for a long time due to factors such as uneven data distribution and poor communication of some clients, this paper introduces the average training time of the local model T_{avg} , see (3). In the s round of training, the convergence time of the local client is T^s . In the first round of training, the initial T_{avg} is the fixed value measured in the experiment, and T_{avg} is the average value of the model training time T^s in the first s round.

$$T_{avg} = \frac{1}{s} \sum_{s=1}^s T^s \tag{3}$$

The aggregation server performs one aggregation operation on all model gradients, and we use the FedAvg aggregation algorithm [2].

$$G^{s+1} \leftarrow \sum_{k=1}^K \frac{D_i}{D} L_i^{s+1} \tag{4}$$

L_i^{s+1} denotes the local model parameters of the i th client at round $s + 1$, and G^{s+1} is the global model update parameter (Table 1).

Table 1. FL-Resnet-CABM central server steps.

Algorithm 1 FL-Resnet-CABM central server steps

- 1: Input: $S, K, G^0, G^s, T^s, Tavg$
- 2: Output: by evaluated the FL- Resnet -CBAM model parameters G^{s+1}
- 3: Create a task and start training
- 4: **for** global model aggregation count s ($1 < s < S$) **do**
- 5: Arbitrarily pick k ($1 < k < K$) clients to federation training
- 6: **for** the k clients selected in parallel to **do**
- 7: Call Algorithm 2 to obtain the current training time T^s and the model parameters of each client at the end of the s th round of training L_i^{s+1}
- 8: **if** ($T^s > Tavg$)
- 9: **then** Send a non-aggregation command to clients
- 10: **else** Send aggregation command to clients
- 11: **end if**
- 12: **end for**
- 13: Global model parameters G^{s+1} are obtained by FedAvg algorithm, see (4)
- 14: **if** (evaluate global model convergence == **true**)
- 15: **then** stop the client model training and send G^{s+1} distributed to all clients which aggregation commands are sent
- 16: **end if**
- 17: **end for**

Considering the discrete distribution of each client in the federal learning framework, the traditional gradient descent algorithm is limited in its learning rate adjustment strategy and easily falls into many local suboptimal solutions, so this paper uses AdaGrad (Adaptive Gradient) optimization algorithm [13].

$$g_{t,i} = \nabla_{\theta} J(\theta_i) \tag{5}$$

$$\theta_{t+1,i} = \theta_{t,i} - \frac{lr}{\sqrt{G_{t,ii} + \epsilon}} \times g_{t,i} \tag{6}$$

$g_{t,i}$ denotes the moment t of θ_i gradient. $G_{t,ii}$ denotes the gradient of the parameter θ_i of the sum of squared gradients (Table 2).

Cross entropy measures the degree of difference between two different probability distributions in the same random variable, and is expressed in machine learning as the difference between the true probability distribution and the predicted probability distribution. The smaller the value of cross-entropy, the better the model prediction.

The Cross Entropy Loss function is often standard with softmax in classification problems. Softmax processes the output so that the predicted values of its multiple classifications sum to 1, and then calculates the loss by cross entropy.

$$Loss = -[y \times \log \hat{y} + (1 - y) \log(1 - \hat{y})] \tag{7}$$

y is the label value 1 or 0, \hat{y} is the probability that the image is predicted to be a new coronary pneumonia image.

Table 2. FL-Resnet-CABM clients steps.

Algorithm 2 FL-Resnet-CABM clients steps

```

1: Input:  $D, D_i, G^{s+1}, i, C, lr, T^s, B, \text{momentum, minibatch}$ 
2: Output: local model parameters evaluated by  $L_i^{s+1}, T^s$ 
3: Get the latest model parameters  $G^{s+1}$  from the server
4: for local model training times  $c(1 < c < C)$  do
5:   Randomly divide  $D_i$  into  $B = D_i / \text{minibatch}$  copies
6:   Get the local model parameters from the previous iteration
7:   for  $b(1 < b < B)$  do
8:     Get the training parameters  $\text{state\_dict}()$  for each layer from  $G^{s+1}$ 
9:     Get the  $lr$  and momentum to initialize the AdaGrad optimization, see (5,6)
10:    Call improved Resnet50 model to start training
11:    Iterate over the data and labels and place them in  $\text{cuda}()$ 
12:    Optimizer clears the gradient  $\text{zero\_grad}()$ 
13:    Cross entropy  $\text{cross\_entropy}$  calculates the loss value, see equation (7)
14:    Model gradient update  $L_c^{b+1}$  based on parameters in the convolution kernel
15:  end for
16: end for
17: Send this round of client training time  $T^s$  to central server
18: if (evaluate local model convergence = true)
19:   then get local model parameters updated  $L_i^{s+1} = L_c^B$  and send it to central server
20: end if

```

4 Experiments and Analysis

4.1 Experimental Environment

See Table 3.

Table 3. Experimental environment.

Parameters	Configuration
CPU	Intel Core i7-11700 @2.5 GHz
Memory	16 GB
Graphics Cards	GeForce RTX 3080 Ti 12 GB
Operating System	Windows 10
Deep Learning Framework	pytorch 1.5.1
Programming Languages	Python 3.6

4.2 Datasets

We used the dataset COVID-19 Chest X-ray Database [14, 15] to conduct the relevant experiments. We selected 2052 COVID-19 positive cases and 2969 normal lung images

considering the model training efficiency and the complexity of data cleaning. The training set consists of 4021 images, 1652 COVID-19 images, and 2369 normal lung images; the test set consists of 1000 images, 400 COVID-19 images, and 600 normal lung images. The image format within this dataset is png with a size of $299 \times 299 \times 3$.

In this paper, we increase the data discrepancy by rotating the images left and right and cropping them at random centers, because the images rotated at large angles will cause some information of the images to be lost, so the images are rotated arbitrarily between 10° and 30° left and right. When the model is trained, an oversampling method is used to have a put-back sampling operation for a small number of image categories, and with this operation method, the impact of data imbalance on the classification model can be reduced, it is necessary to resize the images in the dataset to change the image size to $224 \times 224 \times 3$.

4.3 Experimental Evaluation Metrics

In this paper, four metrics, Accuracy (Acc), Precision (Prec), Sensitivity (Sen), and Specificity (Spec), are used to evaluate the model for image classification (Table 4):

Table 4. Experimental evaluation index.

Evaluation indicators	Prediction Category	Real Category
True Positive (TP)	COV	COV
True Negative (TN)	Nor	Nor
False Positive (FP)	COV	Nor
False Negative (FN)	Nor	COV

$$Acc = \frac{TP + TN}{Total}$$

$$Prec = \frac{TP}{TP + FP}$$

$$Sen = \frac{TP}{TP + FN}$$

$$Spec = \frac{TN}{FP + TN}$$

4.4 Experimental Results

4.4.1 Ablation Experiments

Ablation experiments were conducted for the average local model training time proposed in this paper, using the average local model training time within the improved model

FL-ResNet-CBAM denoted as Model A and not using average local model training time denoted as Model B. A total of 10 training sessions were conducted. The training was unfolded with all other training conditions being consistent. The number of global model training sessions and the corresponding convergence times are shown in Fig. 5.

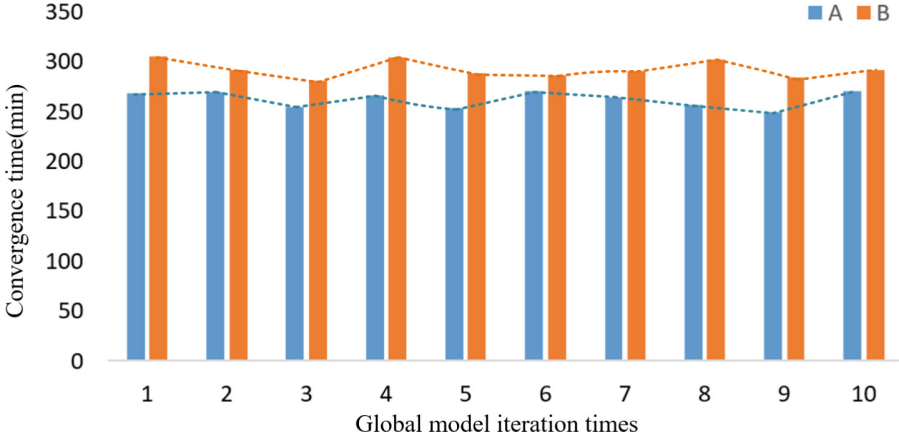


Fig. 5. Convergence time corresponding to the number of training times for Model A and Model B

As can be seen in Fig. 5, the convergence time trend line of model A is lower than that of model B. The average convergence time of model A in 10 global training sessions is 262.3 min, and the average convergence time of model B in 10 global training sessions is 292.5 min, which takes 30.3 min more than model A. It can be seen from the results that the average training time of the local model significantly reduces the convergence time of the global model, which proves the effectiveness of the proposed method.

4.4.2 Comparison Experiments

We designed relevant experiments to test the performance of the proposed model according to the following experimental parameters: $N = 10$, $k = 3$, $C = 3$, $S = 20$, minibatch = 16, and $lr = 0.001$. During training, the local training set of the client is randomly divided, it can satisfy the principle of non-independent identical distribution.

In this paper, the VGG16, ResNet18, and ResNet50 models from the VGG [16] and ResNet [11] networks, as well as the ResNet50-SE, a model incorporating the attention module of the SE channel based on ResNet50, and the FL-ResNet50, an improved model of ResNet50 under the federal learning framework, were selected to compare with the proposed method in this paper in the same. The prediction results of these six models on the test set are shown in Table 5.

As can be seen from the table, comparing VGG16, ResNet18, ResNet50 can be seen that the model in deepening the depth of at the same time, the model accuracy, precision, sensitivity, specificity are improved, in the residual network, although the number of convolutional layers is increased, but due to the existence of residual units, so that part

Table 5. Comparison of the prediction results of FL-ResNet-CBAM and other models.

Models	Acc	Prec	Sen	Spec
VGG16	0.857	0.850	0.78	0.908
ResNet18	0.871	0.861	0.808	0.913
ResNet50	0.883	0.864	0.840	0.912
FL-ResNet50	0.879	0.868	0.823	0.917
ResNet50-SE	0.914	0.901	0.883	0.935
FL-ResNet-CBAM	0.939	0.921	0.928	0.947

of the convolution that does not provide positive feedback is not counted in the results, so The relevant performance results of ResNet50 are higher than those of ResNet18, but not too far apart, and after adding the SE module on the basis of ResNet50, the learning of the model in terms of channels is enhanced, which makes the feature acquisition more comprehensive, and thus the performance of the ResNet50-SE model achieves a comprehensive surpassing of the traditional VGG and ResNet models.

By applying the ResNet50 model to the federal learning framework to achieve the purpose of privacy protection, but from Table 5, we can see that the accuracy and specificity of the FL-ResNet50 model have a small improvement compared with the ResNet50 model, while the accuracy and sensitivity of have decreased, which indicates that the application of deep learning models to the federal learning framework does not necessarily lead to an improvement in all aspects of the model. This suggests that the application of deep learning models in the federal learning framework does not necessarily improve the performance of all aspects of the model, and even degrades some of the performance. This paper argues that this is part of the limitations of federal learning, which may sacrifice a small amount of accuracy at the expense of a significant increase in security.

The FL-ResNet-CBAM model incorporating the CBAM module proposed in this paper achieves both improved prediction results related to the model while using the federal learning framework to ensure security, and all metrics of the FL-ResNet-CBAM model are higher than those of other models, comparing with the FL-ResNet50 model that also uses the federal learning framework, its accuracy and sensitivity are significantly improved compared with the The accuracy and sensitivity of the FL-ResNet50 model are 6 and 10.5 percentage points higher than those of the FL-ResNet50 model, respectively, showing that the CBAM module, which focuses on both channel and spatial information, can achieve the accuracy, precision, sensitivity, and specificity of new coronary pneumonia image classification. This shows that the performance of the model does not degrade under the federal learning framework, but the learning of only the channel information and the lack of spatial information will lose some of the model performance.

During the 20 rounds of global model training, the relationship between the accuracy of each model with increasing number of global iterations is shown in Fig. 6. To show

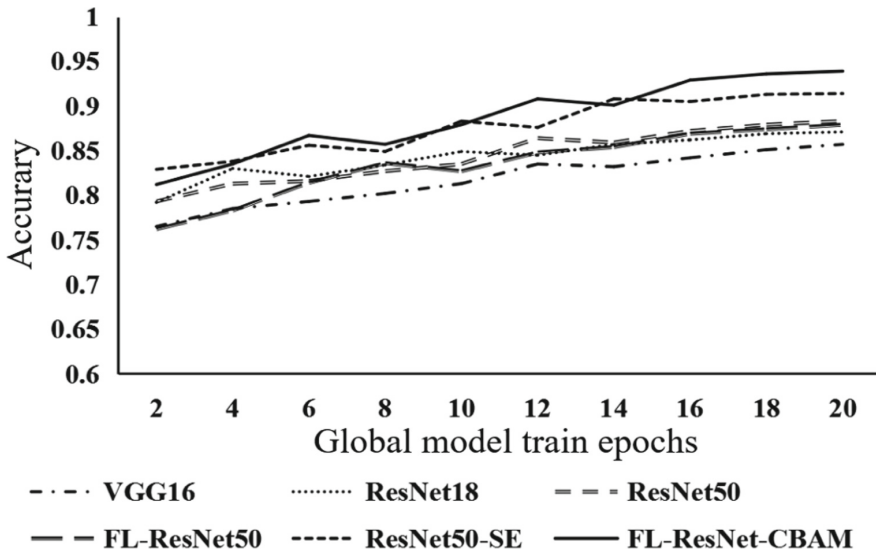


Fig. 6. Relationship between global model train epochs and accuracy of each model

more clearly the difference of accuracy curves of each model in the longitudinal direction, the accuracy starting point of the vertical axis of Fig. 6 is placed at 0.6.

The training process of FL-ResNet-CBAM model is relatively smooth and converges faster than other models, which is partly due to the fact that the federal learning model itself is a distributed model, the new model distributed under each round of client aggregation is normalized, and the local model average training time is used, which allows the model to converge faster.

5 Discussion

In this paper, by improving the residual network ResNet50 under the federal learning framework and adding the hybrid domain attention mechanism, we achieve the improvement of the accuracy, precision, sensitivity, and specificity of the classification of X-ray images of neocoronary pneumonia, and introduce the average training time of the local model in the server-client model training, which solves the problem that the local model does not converge for a long time causing the global model to be unable to converge. The use of AdaGrad optimizer to achieve more efficient model convergence under discrete clients using the information of sparse gradients, and the use of federated learning for distributed training ensures the privacy of medical data and has the advantage of breaking data silos, fully demonstrate the advantages and innovations of the improved algorithm proposed in this paper for new coronary pneumonia detection. In the next work, we consider applying federal learning to more scenarios of detection to break the data barriers while improving the detection accuracy.

References

1. Wong, H.Y.F., et al.: Frequency and distribution of chest radiographic findings in patients positive for COVID-19. *Radiology* **296**(2), E72–E78 (2020)
2. McMahan, B., Moore, E., Ramage, D., Hampson, S., Arcas, B.A.: Communication-efficient learning of deep networks from decentralized data. In *Artificial Intelligence and Statistics*, pp. 1273–1282. PMLR (2017)
3. Psychoula, I., et al.: A deep learning approach for privacy preservation in assisted living. In: *2018 IEEE International Conference on Pervasive Computing and Communications Workshops (PerCom Workshops)*, pp. 710–715. IEEE (2018)
4. Psychoula, I., Chen, L., Amft, O.: Privacy risk awareness in wearables and the internet of things. *IEEE Pervasive Comput.* **19**(3), 60–66 (2020)
5. Yao, X., Farha, F., Li, R., Psychoula, I., Chen, L., Ning, H.: Security and privacy issues of physical objects in the IoT: challenges and opportunities. *Digit. Commun. Netw.* **7**(3), 373–384 (2021)
6. Pfohl, S.R., Dai, A.M., Heller, K.: Federated and differentially private learning for electronic health records. arXiv preprint [arXiv:1911.05861](https://arxiv.org/abs/1911.05861) (2019)
7. Dayan, I., et al.: Federated learning for predicting clinical outcomes in patients with COVID-19. *Nat. Med.* **27**(10), 1735–1743 (2021)
8. Feki, I., Ammar, S., Kessentini, Y., Muhammad, K.: Federated learning for COVID-19 screening from chest X-ray images. *Appl. Soft Comput.* **106**, 107330 (2021)
9. Zhang, W., et al.: Dynamic-fusion-based federated learning for COVID-19 detection. *IEEE Internet Things J.* **8**(21), 15884–15891 (2021)
10. Liu, B., Yan, B., Zhou, Y., Yang, Y., Zhang, Y.: Experiments of federated learning for covid-19 chest x-ray images. arXiv preprint [arXiv:2007.05592](https://arxiv.org/abs/2007.05592) (2020)
11. He, K., Zhang, X., Ren, S., Sun, J.: Deep residual learning for image recognition. In: *Proceedings of the IEEE Conference on Computer Vision and Pattern Recognition*, pp. 770–778 (2016)
12. Woo, S., Park, J., Lee, J.-Y., Kweon, I.S.: CBAM: convolutional block attention module. In: Ferrari, V., Hebert, M., Sminchisescu, C., Weiss, Y. (eds.) *ECCV 2018*. LNCS, vol. 11211, pp. 3–19. Springer, Cham (2018). https://doi.org/10.1007/978-3-030-01234-2_1
13. Duchi, J., Hazan, E., Singer, Y.: Adaptive subgradient methods for online learning and stochastic optimization. *J. Mach. Learn. Res.* **12**(7), 261 (2011)
14. Rahman, T., et al.: Exploring the effect of image enhancement techniques on COVID-19 detection using chest X-ray images. *Comput. Biol. Med.* **132**, 104319 (2021)
15. Chowdhury, M.E., et al.: Can AI help in screening viral and COVID-19 pneumonia? *IEEE Access* **8**, 132665–132676 (2020)
16. Simonyan, K., Zisserman, A.: Very deep convolutional networks for large-scale image recognition. arXiv preprint [arXiv:1409.1556](https://arxiv.org/abs/1409.1556) (2014)